Phased Array Antenna Beam-Steering in a Dispersion-Engineered Few-Mode Fiber

Elham Nazemosadat, Jose I. Herranz-Herruzo, *Member, IEEE*, and Ivana Gasulla, *Senior Member, IEEE*

***Abstract*—We present, for the first time to our knowledge, experimental demonstration of tunable optical beamforming for phased array antennas using a few-mode fiber. The double-clad step-index few-mode fiber is dispersion engineered such that it operates as a continuously tunable 5-sample true-time delay line, enabling continuous steering of the beam-pointing angle. Using this approach, we measure the radiation pattern from 5 elements of an in-house fabricated 8-element phased array antenna at the radiofrequency of 26 GHz and demonstrate continuous beam-steering over a 59° range by sweeping the optical wavelength from 1543 nm up to 1560 nm. Such a few-mode fiber-based beamformer could be beneficial to next-generation fiber-wireless communications and radar systems, as it provides further versatility and capacity along with reduced size, weight and power consumption.**

***Index Terms*—Beam steering, few-mode fibers, microwave photonics, phased array antennas, space division multiplexing.**

I. Introduction

BEAMFORMING for phased array antennas (PAAs) is a key technology in radar and wireless communications systems, enabling the shaping and steering of beams towards specific directions. Traditional analog beam-steering techniques based on phase shifters are prone to beam squinting, and therefore unsuitable for wideband operation [1]. To address this issue, true-time delay lines (TTDLs) are often used instead, as they introduce frequency-independent delays and thereby accommodate broadband beamforming [2]. Optical approaches are considered as the most promising technology to realize TTDLs, as they offer immunity to electromagnetic interference, along with a broader bandwidth and lower losses compared to their electronic counterparts [3].

Different schemes have been used to develop optical TTDL beamformers, including those based on dispersive fibers [4], fiber Bragg gratings [5], stimulated Brillouin scattering [6], optical ring resonators [7], and subwavelength grating waveguides [8], among others. Moreover, multicore (MCF) and few-mode fibers (FMFs), which have found applications in various fields such as optical transmission [9], imaging [10], sensing [11] and nonlinear switching [12], have also proven useful to microwave photonics signal processing [13]. In the context of microwave photonics, the parallelism inherent to the spatial dimension of these fibers can be used to implement TTDLs [14], [15], [16], and therefore, allow simultaneous distribution and processing of microwave signals within the same fiber link. This approach, which eliminates the need for an external device to process the signal, particularly gains importance in scenarios where the radio-over-fiber link is required anyway. Moreover, taking advantage of the spatial diversity in MCFs and FMFs makes it possible to use only one laser source, while other fiber-based TTDLs that exploit optical wavelength diversity require several lasers [4], [5]. Recently, this scheme was used to demonstrate a TTDL beamformer for PAAs in a custom dispersion-engineered heterogeneous MCF [17]. A few beamforming networks using FMFs have also been reported so far [18], [19], [20]. However, their main drawback is that the tunable TTDL operation is not solely provided by the FMF and external delay control is required by either changing the FMF length [18], using FMF Bragg gratings [19], or employing optical switches [19], [20]. We have recently proposed [21] and experimentally demonstrated [16] a dispersion-tailored FMF that overcomes this limitation by acting as a tunable TTDL, offering continuous time-delay tunability over a broad range through varying the optical wavelength. Here, we use this FMF-based TTDL to realize an optical beamforming network. To the best of our knowledge, this is the first experimental demonstration of tunable optical beamforming for PAAs using a FMF, where the FMF itself provides the required tunable TTDL operation, making the system reconfigurable and yet simple. Such a scheme, which allows simultaneous processing and distribution of microwave signals, could be particularly interesting for next-generation wireless communications systems, such as Beyond 5G, as it offers increased versatility, capacity and compactness.

Manuscript received 26 April 2023; revised 20 June 2023; accepted 30 June 2023. Date of publication 5 July 2023; date of current version 2 November 2023. This work was supported in part by the ERC Consolidator under Grant 724663, in part by Spanish Ministerio de Ciencia e Innovación Project under Grant PID2020-118310RB-100, and in part by Generalitat Valenciana under Grants IDIFEDER/2018/031 and PROMETEO/2021/15. *(Corresponding author: Elham Nazemosadat.)*

The authors are with the Institute of Telecommunications and Multimedia (ITEAM), Universitat Politècnica de València, 46022 Valencia, Spain (e-mail: sbnazars@iteam.upv.es; jiherhe@upvnet.upv.es; ivgames@iteam.upv.es).

Color versions of one or more figures in this article are available at https://doi.org/10.1109/JLT.2023.3292509.

Digital Object Identifier 10.1109/JLT.2023.3292509

II. Few-Mode Fiber True-Time Delay Line

The different spatial modes of a FMF have distinct group delays and propagate at different velocities in the fiber. Therefore, at the FMF output, different time-delayed replicas of an input signal are provided by the different modes. We can utilize this property to implement a tunable TTDL. In this case, through custom fiber design, two specific conditions should be met. First, the dispersion properties of the modes must be tailored such

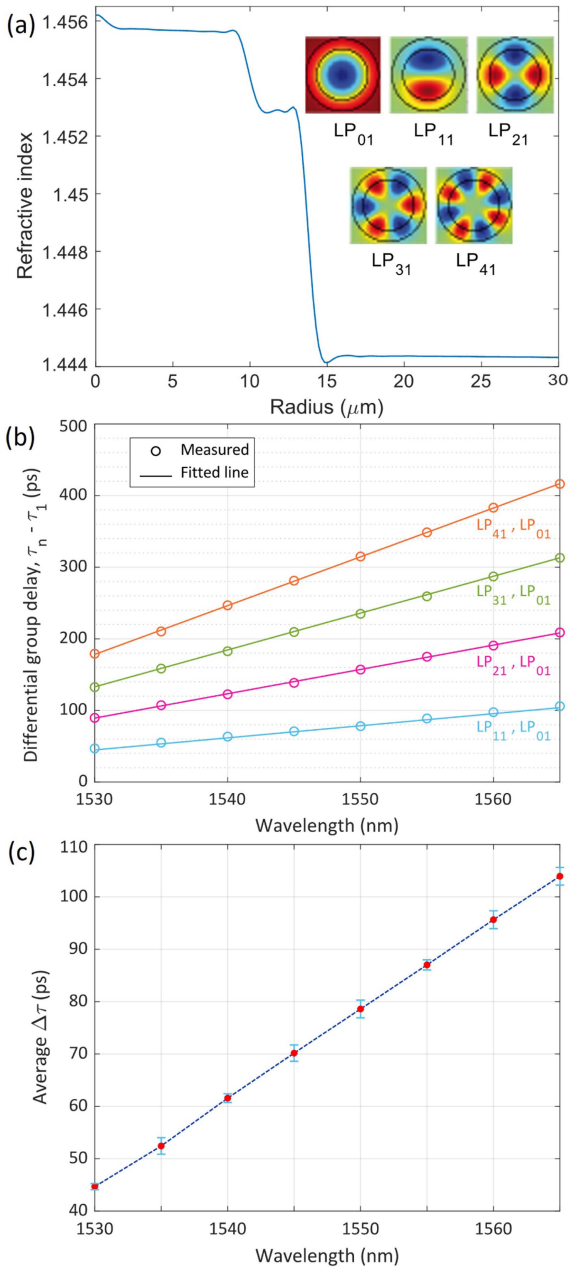

Fig. 1. (a) Refractive index profile of the developed double-clad step index FMF at 1550 nm along with the transverse mode profiles of the 5 modes of interest that are suitable for true-time delay line operation. (b) Differential group delays of the modes of interest, with respect to LP_{01}. The circles represent measured data, while the solid lines are the fitted trend lines. (c) Measured (red dots) and fitted (dotted blue line) values for the average $\Delta\tau$. The corresponding error bars for the measured values are also shown.

that the differential time delay $\Delta\tau$ between adjacent replicas (or the differential group delay (DGD) between adjacent modes) is constant at a given wavelength. Second, to obtain continuous delay tunability, $\Delta\tau$ should vary linearly with the optical wavelength, which means that the differential dispersion slope between adjacent modes should be minimized.

In mathematical terms, the group delay of spatial mode n, can be expanded in a 1-st order Taylor series around an anchor

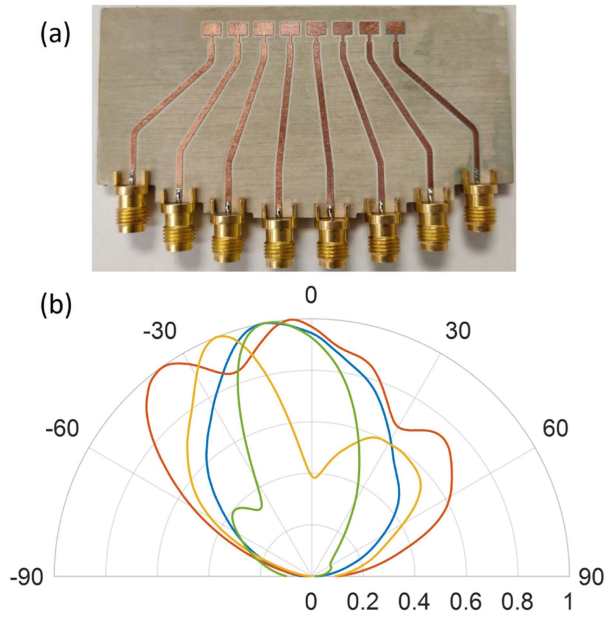

Fig. 2. (a) The in-house built 8-element phased array antenna. (b) Radiation pattern of a single antenna element, measured for 4 different individual elements.

wavelength λ_0, as

$$\tau_n(\lambda) = \tau_{0,n} + (\lambda - \lambda_0) D_n L \tag{1}$$

where $\tau_{0,n}$ and D_n indicate the group delay and chromatic dispersion of mode n at λ_0, respectively, and L is the fiber length. When exploiting the space dimension, the basic time delay among adjacent samples at a particular wavelength is given by the differential group delay between each pair of adjacent modes, expressed as $\Delta\tau(\lambda) = \tau_n(\lambda) - \tau_{n-1}(\lambda)$. If the FMF is designed such that all modes have the same group delay at the anchor wavelength (identical $\tau_{0,n}$ value), then we have

$$\Delta\tau(\lambda) = (\lambda - \lambda_0)\Delta D L \tag{2}$$

where $\Delta D = D_n - D_{n-1}$ is the differential chromatic dispersion between neighboring modes. Based on (2), to fulfill the two above-mentioned conditions for tunable TTDL operation, ΔD should be constant [21].

Considering these requirements, we have recently developed a few-mode fiber with a double-clad step-index profile that features relatively evenly-spaced incremental chromatic dispersion values of $\Delta D = 1.7$ ps/nm/km among 5 of its linearly polarized (LP) modes, namely, LP_{01}, LP_{11}, LP_{21}, LP_{31} and LP_{41}. The modal crosstalk is minimized among these modes as they belong to different mode-groups. Fig. 1(a) shows the refractive index profile of the 1-km long FMF, fabricated by YOFC company, where the radii of its silica core, inner and outer claddings are 9.1, 13 and 62.5 μm, while their GeO_2 doping concentrations are 7.79, 5.93, and 0.22 mol%, respectively. The measured differential group delays of the modes with respect to LP_{01} are displayed in Fig. 1(b), where for every wavelength, we can see that the group delay increases in constant steps as the mode number increases. The average $\Delta\tau$ value among neighboring modes at different wavelengths, together with its standard deviation is

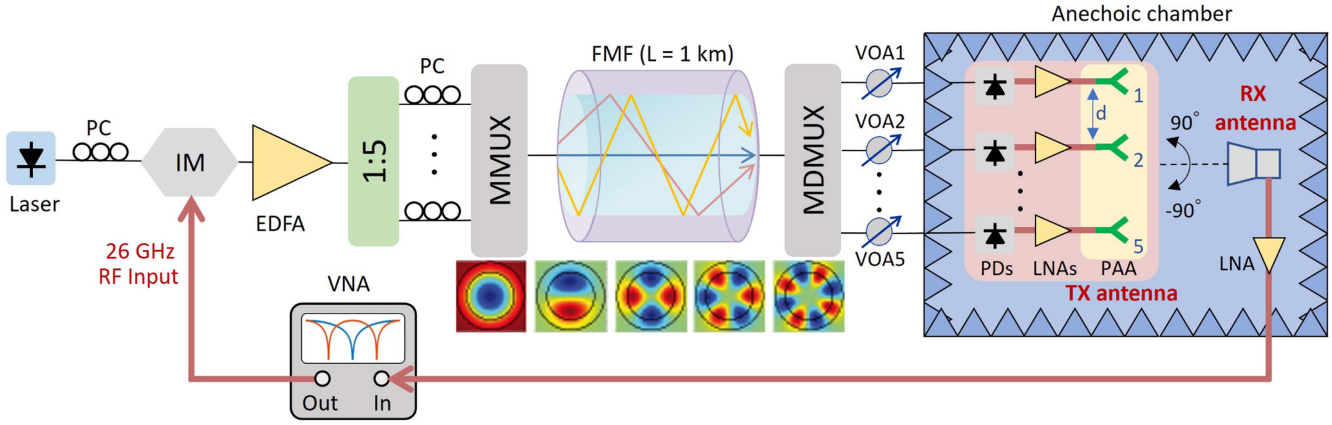

Fig. 3. Experimental setup used for measuring the radiation pattern of the optical beamforming network. PC: polarization controller, IM: intensity modulator, EDFA: erbium-doped fiber amplifier, MMUX (MDMUX): mode (de)multiplexer, VOA: variable optical attenuator, PD: photodetector, LNA: low-noise amplifier, PAA: phased array antenna.

depicted in Fig. 1(c). It clearly shows that $\Delta\tau$ increases linearly with the optical wavelength in the 35-nm wavelength range of the optical C-band, indicating that the developed FMF can operate as a continuously tunable TTDL.

III. Phased Array Antenna

Phased array beamforming is obtained when a constant time delay of $\Delta\tau$ is introduced between the microwave signals radiating from the antenna elements, corresponding to a progressive phase shift of $\Delta\phi = 2\pi f_{RF}\Delta\tau$ among them, where f_{RF} is the operating radiofrequency (RF). The total radiation pattern from an PAA is the radiation pattern from a single-element, known as the element factor, multiplied by an array factor (AF). The AF, which is dependent on the geometry of the array and the excitation of the elements in terms of amplitude and phase, is given by [22]

$$AF(\theta) = \frac{1}{N}\sum_{n=0}^{N-1} a_n e^{j2\pi f_{RF} n(\Delta\tau + dsin(\theta)/c)} \qquad (3)$$

where θ is the far field angular coordinate, N is the number of radiating elements, a_n represents the amplitude of the signal radiated by element n, d is the spacing between the antenna elements, and c is the speed of light in vacuum. As we can understand from (3), the beam-pointing angle, at which the maximum radiation occurs, depends on $\Delta\tau$. Thus, when using our developed FMF-based TTDL to implement a beamformer for PAAs, the beam can be steered by changing the differential group delay among the spatial modes, which we can realize by simply varying the operational optical wavelength, as seen in Fig. 1(c).

A microstrip PAA, with 8 elements separated by $d = 5.77$ mm ($\lambda_{RF}/2$ at 26 GHz), was designed and fabricated at our facilities, using a milling machine on a substrate Rogers RT5880 with a height of 0.381 mm and relative permittivity of 2.2. A picture of the fabricated 8-element PAA is illustrated in Fig. 2(a). The measured radiation patterns of 4 representative antenna elements are displayed in Fig. 2(b). These patterns, which should ideally be similar, are very different and have considerable power variations. This non-uniformity affects the total radiation pattern from the PAA, as will be discussed in the following sections.

IV. Optical Beamforming Experimental Setup and Results

We use our developed FMF-based TTDL to experimentally demonstrate 5-element optical beamforming for the PAA, using the setup of Fig. 3. The optical signal from a tunable laser is intensity modulated by a 10 dBm RF signal at 26 GHz, generated by a vector network analyzer (VNA). The modulated signal is amplified and split into 5 paths. After controlling the polarization, the signal in each path is injected into one of the 5 modes of interest (LP_{01}, LP_{11}, LP_{21}, LP_{31} and LP_{41}) of the 1-km FMF using a mode multiplexer. After propagating through the FMF, the signals are extracted from the modes using a demultiplexer. The multiplexer/demultiplexer pair are fabricated by Cailabs, with an average back-to-back modal crosstalk and average insertion loss of -19 dB and 9.3 dB at 1565 nm, respectively. Among every two degenerate asymmetrical LP_{lm} modes ($l \geq 1$), the power from only one of them is collected. Thus, we maximize the power in that specific mode using the polarization controller placed before the multiplexer. The variations in its power, caused by the inevitable mode coupling with the other degenerate mode can also be controlled using this approach. At the FMF output, the powers coming from the different modes are equalized using variable optical attenuators. The 5 optical signals are then directed to an anechoic chamber, where each one is detected by an individual photodiode and converted back to the electrical domain. After amplifying the RF signals, they are fed into 5 consecutive elements of the 8-element PAA. For measuring the radiation patterns, the PAA is mounted on an antenna positioner that is capable of 180-degree azimuth rotation. The received power is measured using a receiver horn antenna, placed 3 meters away from the transmitter antenna. The power is then amplified by a low-noise amplifier (LNA) and the

radiation pattern is measured by the VNA. Beam-steering is realized by sweeping the optical wavelength of the laser.

Using (3) and the DGD values extracted from the fitted lines of Fig. 1(b), the normalized radiation patterns and beam-pointing angles for different wavelengths are calculated and illustrated in Fig. 4(a) and (b), respectively. The results indicate that theoretically, beam-steering from approximately -90° to 90° could be achieved. However, as seen in Fig. 4(a), the farther the angle is from broadside direction, the main lobe becomes broader and the main-to-side-lobe ratio (MSLR) decreases; thus, limiting the operational range. Additionally, in practice, the beam-steering range is restricted by the characteristics of the single-element radiation patterns, which have significant variations from one another.

To evaluate the performance of the FMF-based beamformer, we vary the optical wavelength from 1543 nm to 1560 nm, corresponding to average time delays between 66.7 ps and 95.6 ps. This steers the beam-pointing angle from 22° down to -37°, as we can see in Fig. 5, where the normalized measured radiation patterns at 8 different wavelengths are displayed. The corresponding beam-pointing angles are shown by red squares in Fig. 4(b). The results show main lobe broadening at angles farther from broadside direction, as expected from the simulations of Fig. 4(a). This can be improved by using a TTDL with a higher number of samples, which could be achieved by increasing the number of modes, but at the expense of an increase in the modal crosstalk. An alternative is to increase the number of samples by using optical lasers with different wavelengths at the input (combining wavelength division multiplexing and space division multiplexing). For example, using two lasers instead of one, would double the number of samples. Another technique would be to use a combination of cores and modes, i.e., a customized multicore fiber in which each core supports a few modes. This way, through proper design, we can ensure a low level of crosstalk among the modes within each core and among different cores.

V. Discussion

In our beamforming experiment, initially the system was optimized to perform the measurements using 5 specific elements of the 8-element PAA. In this case, the beam-pointing angle had good agreement with the theoretical values at different wavelengths, but in some cases high power was observed in the side-lobes, decreasing the MSLR. As Fig. 4(c) shows, this is due to non-uniform power distribution among the 5 signals. Even though before starting the measurements, the powers of the signals radiated from the elements were equalized, their power distribution varied throughout the measurements at different beam-pointing angles, which is mostly attributed to the considerably different power levels of the single-element radiation patterns. Therefore, to achieve uniform power distribution, it was necessary to make up for the element factor variations at every step, which required a lot of time and was not feasible for us. Hence, to reduce the effect of the dissimilar element radiation patterns, for steering the beam to a specific beam-pointing angle, rather than using a fixed set of antenna elements, we chose the 5 consecutive elements whose radiation patterns were least different at that particular angle. For example, for steering the beam to -30°, according to Fig. 2(b), we avoided the element whose radiation pattern is shown in green, as it experiences a significant power drop at this angle. This notably improved the

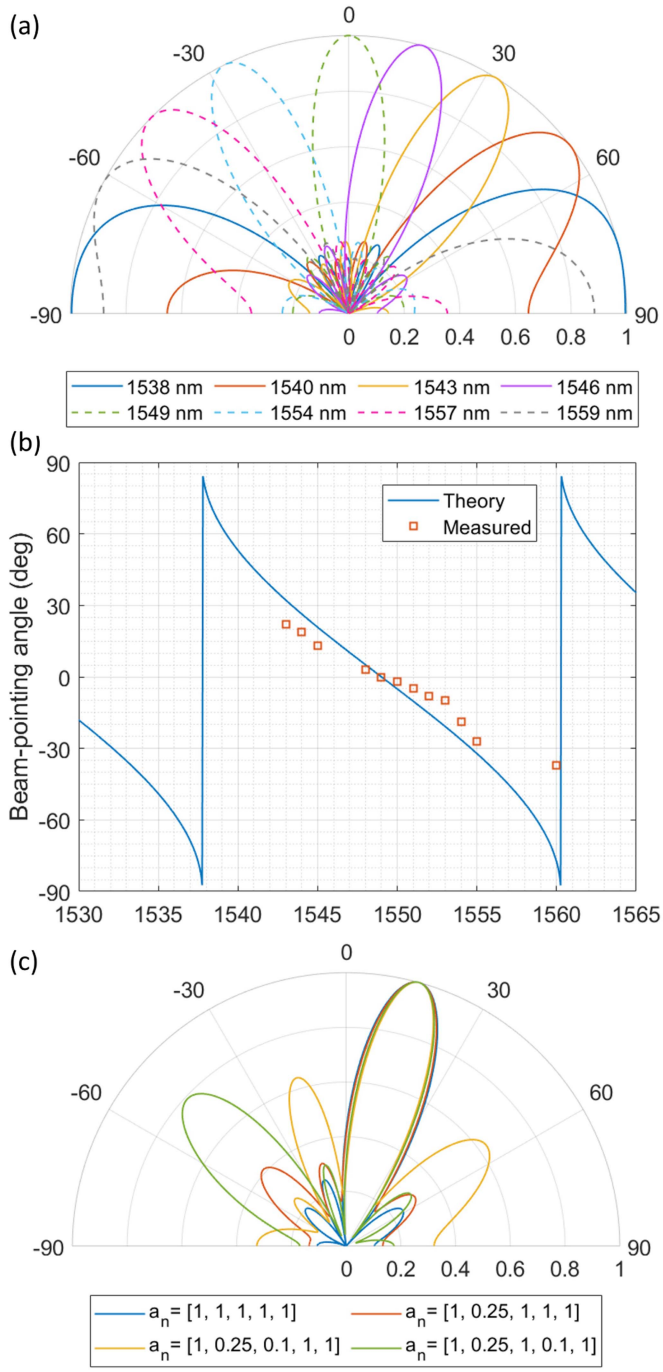

Fig. 4. (a) Simulated radiation patterns of the phased array antenna at different wavelengths. The DGD values extracted from the fitted lines of Fig. 1(b) are used to perform these simulations. (b) Variations of the beam-pointing angle (shown in degrees) with the optical wavelength, found through simulations (blue line) and measurements (red squares). (c) Simulated radiation patterns of the phased array antenna with different input power distributions (a_n is the normalized amplitude of the signal fed to each of the 5 elements).

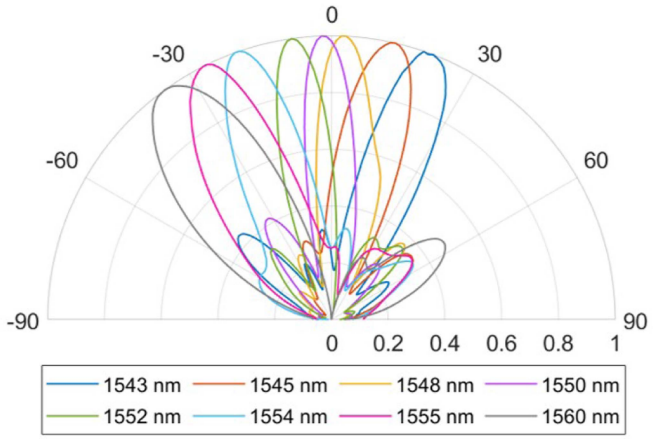

Fig. 5. Radiation patterns of the phased array antenna, measured at different optical wavelengths at an RF operating frequency of 26 GHz.

MSLR compared to the case where a fixed set of elements were used for all angles. However, the downside of this approach is that using different elements for different angles introduces slight variations to the electrical paths of the 5 signals, leading to minor changes in the time delay $\Delta\tau$ among them. According to (3), this causes a shift in the beam-pointing angle, explaining the offset observed among theoretical and measured values of Fig. 4(b). Employing a PAA that exhibits better performance in terms of its element radiation patterns would overcome these issues and further improve our results in terms of steering range and MSLR. Nonetheless, our results show the applicability of a FMF-based TTDL in tunable beamforming for a PAA. Moreover, besides the single-element radiation patterns, which we believe are the main restriction in this experiment, minor variations in $\Delta\tau$ between neighboring modes could cause a slight shift in the beam-pointing angle. Also, coupling between the modes could affect the power distribution among the signals and reduce the MSLR. However, for several wavelengths, we repeated the experiment after 10 minutes and quite similar results were obtained, even though the FMF spool was not placed on a vibration isolating table. This indicates that the linear mode coupling did not notably affect the radiation patterns. Keeping the FMF spool in a controlled environment would reduce the effect of external coupling sources.

VI. Conclusion

We experimentally present continuously tunable optical beamforming for a phased array antenna using a 1-km few-mode fiber link. To the best of our knowledge, this is the first-ever demonstration in which the FMF itself provides the tunable time delay required for beam-steering, without requiring external delay control. This was made possible by the unique dispersion properties of the custom-designed double-clad step-index FMF, which allowed it to operate as a tunable sampled true-time delay line. The 5-element radiation pattern of a PAA is measured in an anechoic chamber at an RF frequency of 26 GHz, where the beam-pointing angle is steered within a 59° range, from 22° to −37°, by sweeping the optical wavelength of the laser from 1543 nm to 1560 nm. The radiation patterns of different individual elements show different behavior, indicating that our in-house fabricated PAA is not ideal. Thus, we believe a wider steering range could be obtained by employing an PAA with improved performance.

Such FMF-based TTDLs offer a promising approach for implementing fiber-distributed signal processing in a compact and versatile manner, where the distribution and processing functionalities are realized simultaneously within the same fiber medium. We have previously demonstrated the applicability of this technique to tunable microwave signal filtering [16]. Arbitrary waveform generation and shaping, as well as time differentiators/integrators are among other signal processing functionalities that could benefit from this approach.

References

[1] I. Frigyes and A. J. Seeds, "Optically generated true-time delay in phased-array antennas," *IEEE Trans. Microw. Theory Techn.*, vol. 43, no. 9, pp. 2378–2386, Sep. 1995.
[2] M. Longbrake, "True time-delay beamsteering for radar," in *Proc. IEEE Nat. Aerosp. Electron. Conf.*, 2012, pp. 246–249.
[3] J. Capmany and D. Novak, "Microwave photonics combines two worlds," *Nature Photon.*, vol. 1, no. 6, pp. 319–330, Jun. 2007.
[4] S. Blanc, M. Alouini, K. Garenaux, M. Queguiner, and T. Merlet, "Optical multibeamforming network based on WDM and dispersion fiber in receive mode," *IEEE Trans. Microw. Theory Techn.*, vol. 54, no. 1, pp. 402–411, Jan. 2006.
[5] Y. Liu, J. Yang, and J. Yao, "Continuous true-time-delay beamforming for phased array antenna using a tunable chirped fiber grating delay line," *IEEE Photon. Technol. Lett.*, vol. 14, no. 8, pp. 1172–1174, Aug. 2002.
[6] S. Chin et al., "Broadband true time delay for microwave signal processing, using slow light based on stimulated Brillouin scattering in optical fibers," *Opt. Exp.*, vol. 18, no. 21, pp. 22599–22613, Oct. 2010.
[7] M. Burla et al., "Integrated photonic k_U-band beamformer chip with continuous amplitude and delay control," *IEEE Photon. Technol. Lett.*, vol. 25, no. 12, pp. 1145–1148, Jun. 2013.
[8] Y. Wang, H. Sun, M. Khalil, L. R. Chen, and W. Dong, "Photonic beamforming based on subwavelength gratings on-chip optical true time delay lines," in *Proc. IEEE Photon. Conf.*, 2020, pp. 1–2.
[9] D. J. Richardson, J. M. Fini, and L. E. Nelson, "Space-division multiplexing in optical fibres," *Nat. Photon.*, vol. 7, no. 5, pp. 354–362, 2013.
[10] Y. Choi et al., "Scanner-free and wide-field endoscopic imaging by using a single multimode optical fiber," *Phys. Rev. Lett.*, vol. 109, Nov. 2012, Art. no. 203901.
[11] Y. Liu and L. Wei, "Low-cost high-sensitivity strain and temperature sensing using graded-index multimode fibers," *Appl. Opt.*, vol. 46, no. 13, pp. 2516–2519, May 2007.
[12] E. Nazemosadat and A. Mafi, "Design considerations for multicore optical fibers in nonlinear switching and mode-locking applications," *J. Opt. Soc. Amer. B*, vol. 31, no. 8, pp. 1874–1878, Aug. 2014.
[13] I. Gasulla and J. Capmany, "Microwave photonics applications of multicore fibers," *IEEE Photon. J.*, vol. 4, no. 3, pp. 877–888, Jun. 2012.
[14] D. V. Nickel, C. Villarruel, K. Koo, F. Bucholtz, and B. Haas, "Few mode fiber-based microwave photonic finite impulse response filters," *J. Lightw. Technol.*, vol. 35, no. 23, pp. 5230–5236, Dec. 2017.
[15] S. García, M. Ureña, and I. Gasulla, "Dispersion-diversity multicore fiber signal processing," *ACS Photon.*, vol. 9, no. 8, pp. 2850–2859, 2022.
[16] E. Nazemosadat and I. Gasulla, "Reconfigurable few-mode fiber-based microwave photonic filter," *J. Lightw. Technol.*, vol. 40, no. 19, pp. 6417–6422, Oct. 2022.
[17] M. Ureña, S. García, J. I. Herranz, and I. Gasulla, "Experimental demonstration of dispersion-diversity multicore fiber optical beamforming," *Opt. Exp.*, vol. 30, no. 18, pp. 32783–32790, Aug. 2022.
[18] M. Zhang, X. Liu, R. Pang, and G. Hu, "Two-dimensional fiber beamforming system based on mode diversity," *IEEE Access*, vol. 9, pp. 35968–35972, 2021.
[19] X. Liu, M. Zhang, P. Zhang, and G. Hu, "2-D beamforming system based on photonic lantern and few-mode fiber Bragg grating," *Opt. Commun.*, vol. 530, 2023, Art. no. 129131.

[20] S. Wang and G. Hu, "A compact beamformer of diversity multiplexing of multiple modes by utilizing few-mode long-period fiber gratings," *Opt. Laser Technol.*, vol. 158, 2023, Art. no. 108879.
[21] E. Nazemosadat and I. Gasulla, "Dispersion-tailored few-mode fiber design for tunable microwave photonic signal processing," *Opt. Exp.*, vol. 28, no. 24, pp. 37015–37025, 2020.
[22] W. Ng, A. A. Walston, G. L. Tangonan, J. J. Lee, I. L. Newberg, and N. Bernstein, "The first demonstration of an optically steered microwave phased array antenna using true-time-delay," *J. Lightw. Technol.*, vol. 9, no. 9, pp. 1124–1131, Sep. 1991.

Elham Nazemosadat received the B.S. degree in electrical engineering from Shiraz University, Shiraz, Iran, in 2006, and the Ph.D. degree in electrical engineering from Nanyang Technological University, Singapore, in 2012. She was a Postdoctoral Researcher with the University of Wisconsin-Milwaukee, Milwaukee, WI, USA, and Chalmers University of Technology, Gothenburg, Sweden. She is currently with Universitat Politècnica de València, Valencia, Spain. Her research interests include applications of multicore and few-mode fibers in microwave photonics, design of specialty fibers, nonlinear Kerr effect in space-division multiplexed fibers for all-optical signal processing, and silicon nitride waveguides, and microresonators.

Jose I. Herranz-Herruzo (Member, IEEE) was born in Valencia, Spain, in 1978. He received the M.S. and Ph.D. degrees in telecommunication engineering from the Universitat Politècnica de València (UPV), Valencia, Spain, in 2002 and 2015, respectively. In 2002, he joined the Antennas and Propagation Laboratory, Institute of Telecommunications and Multimedia Applications, UPV. In 2005, he became an Assistant Professor and he has been an Associate Professor with the Communications Department, UPV, since 2019. His research interests include the numerical modeling and design of waveguide slot arrays and the application of gap waveguide technology to the design of microwave and millimeter-wave antennas and components.

Ivana Gasulla (Senior Member, IEEE) received the M.Sc. degree in telecommunications engineering and the Ph.D. degree in telecommunications from the Universitat Politècnica de València (UPV), Valencia, Spain, in 2005 and 2008, respectively. She is currently an Associate Professor with UPV. From 2012 to 2014, she was a Fulbright Scholar with Stanford University, Stanford, CA, USA. Her research interests include the application of multimode and multicore fibers to Microwave Photonics systems. The results of her work have led to more than 125 international publications, highlighting contributions to Nature Communications and Nature Photonics. In 2017, she was awarded a prestigious ERC Consolidator Grant to develop new Space-Division Multiplexing technologies for emergent fiber-wireless communications through the project InnoSpace. She is/has been a Member of the TPC of the most prestigious conferences in the field, such as the Optical Fiber Communication Conference and European Conference on Optical Communications. She is the Senior Editor of IEEE JOURNAL OF SELECTED TOPICS IN QUANTUM ELECTRONICS and an Associate Editor for IEEE PHOTONICS TECHNOLOGY LETTERS, among others.